Pharm Res (2015) 32:2973–2982
DOI 10.1007/s11095-015-1679-1

RESEARCH PAPER

Characterization of efflux transport proteins of the human choroid plexus papilloma cell line HIBCPP, a functional *in vitro* model of the blood-cerebrospinal fluid barrier

Alexandra Bernd[1] • Melanie Ott[1] • Hiroshi Ishikawa[2] • Horst Schroten[3] • Christian Schwerk[3] • Gert Fricker[1]

Received: 19 November 2014 / Accepted: 18 March 2015 / Published online: 19 May 2015

ABSTRACT

Purpose To characterize the human choroid plexus (CP) papilloma cell line HIBCPP with respect to ABC export protein expression and function in order to evaluate its use as an *in vitro* model to study carrier-mediated transport processes at the CP.

Methods Expression profiles of ABC transporters were studied by quantitative real-time PCR and Western Blot analysis. Functionality of transporters was investigated by means of uptake experiments and permeation studies carried out on permeable filter systems. In addition, immunohistochemistry served to study localization of ABCC1 and ABCC4.

Results Both qPCR and Western Blot revealed that ABC transporters known to be expressed in CP are also expressed in HIBCPP cells. Immunohistochemistry confirmed basolateral expression of ABCC1. Functionality of ABCC1, ABCC4, ABCB1 and ABCG2 could be shown in uptake assays.

Conclusions Altogether, the HIBCPP cells promise to be a functional and relevant *in vitro* tool to investigate transport processes at the blood-cerebrospinal fluid barrier.

KEY WORDS ABC transporter · barrier function · blood-cerebrospinal fluid barrier · HIBCPP · human cell line

Gert Fricker and Christian Schwerk share senior authorship.

✉ Gert Fricker
gert.fricker@uni-hd.de

[1] Institute of Pharmacy and Molecular Biotechnology, Ruprecht-Karls University Heidelberg, Im Neuenheimer Feld 329 69120 Heiderlberg, Germany

[2] Department of NDU Life Sciences, Nippon Dental University, School of Life Dentistry, Tokyo, Japan

[3] Pediatric Infectious Diseases, Department of Pediatrics, Medical Faculty Mannheim, Heidelberg University, Mannheim, Germany

ABBREVIATIONS

ABC	ATP-binding cassette
BCRP	Breast cancer resistance protein
BCSFB	Blood-cerebrospinal fluid barrier
CP	Choroid plexus
CSF	Cerebrospinal fluid
KRB	Krebs Ringer Buffer
MRP	Multidrug resistance-associated protein
P-GP	P-glycoprotein
qPCR	Quantitative real-time PCR
TEER	Transepithelial electrical resistance
ZO-1	Zonula occludens protein 1

INTRODUCTION

The blood-cerebrospinal fluid (CSF) barrier (BCSFB) is – besides the blood–brain barrier – responsible for maintenance of homoeostasis in the brain. The morphological structure of the BCSFB is built up by the epithelial cells of the choroid plexus (CP) producing the CSF. These cells are interconnected by tight junctions which inhibit free paracellular diffusion of substances from blood to CSF (1). Nevertheless, transport of substances from blood to CSF and vice versa is mediated by several membrane proteins (2). The CP consists of four parts being localised in both lateral ventricles, in the third and the fourth ventricle (1). There are some primary CP epithelial cell models used for *in vitro* experiments, inter alia a porcine model which provides high transepithelial electrical resistance (TEER) values and can thus be used for transport studies on permeable filter systems (3). However, preparation of primary cells is time-consuming and costly. Recently, an immortal porcine CP epithelial cell line has been described, but only preliminarily characterized for expression of transport proteins (4). Furthermore, rodent CP epithelial cell lines were established (5, 6) but their use for transport studies is limited (7). Especially, a human CP epithelial cell line model

presenting a function barrier as well as transport properties would be an important tool for pharmacological studies at the BCSFB. HIBCPP cells were obtained from a CP papilloma of the lateral ventricle from a 29-year-old woman (8) and have been established as a functional model of the BCSFB presenting a high TEER and low permeability for macromolecules (9). Subsequently, HIBCPP cells have been used as an *in vitro* model of the BCSFB to analyse origin and development of bacterial and viral meningitis (9–13). Still, the HIBCPP cell line has not yet been characterized with respect to transport protein expression and function, preventing an assessment concerning their suitability for pharmacological research.

The ATP-binding cassette (ABC) transporter family plays a pivotal role in restricting xenobiotics to enter the brain. Several of these transporters are expressed in CP epithelial cells: ABCC1 (multidrug resistance-associated protein 1, MRP1), ABCC2 (MRP2), ABCC3 (MRP3), ABCC4 (MRP4), ABCC5 (MRP5), ABCC6 (MRP6), ABCB1 (P-glycoprotein, P-GP) and ABCG2 (breast cancer resistance protein, BCRP) (14–16). The efflux transporters ABCC1 and ABCC4 are located at the basolateral membrane (blood side) and exhibit a broad substrate specifity (17–21). Substrates of ABCC1 include fluorescein methotrexate (22) and sulforhodamine 101 (23), substrates of ABCC4 are cyclic nucleotides cAMP and cGMP, adefovir and topotecan (19). Moreover, fluo-cAMP (a fluorescein-linked cAMP analogue) transport is mediated by this transporter (24). Both, ABCC1 and ABCC4 can be inhibited with MK 571. The localization of ABCB1 is found to be subapical and intracellular in CP epithelial cells (18, 20). Calcein AM (calcein acetoxymethyl ester), digoxin and rhodamine 123 are among its substrates, and it is inhibited by cyclosporine A, GF 120918 and PSC 833 (Valspodar) (17, 25). ABCG2 is expressed at the apical membrane in CP (15). Substrates include mitoxantrone and BODIPY® (FL) prazosin (17, 26) and it is specifically inhibited by fumitremorgin C and Ko134 (26, 27).

In this study, we have characterized the expression and functionality of efflux transporters in HIBCPP cells and evaluate the use of this cell line as *in vitro* model to study transport at the BCSFB.

MATERIALS AND METHODS

Materials

Dulbecco's Modified Eagle Medium: Nutrient Mixture F-12 (DMEM/F-12) and fetal bovine serum (FBS) were obtained from Life Technologies (Darmstadt, Germany); penicillin/streptomycin and L-glutamine from Biochrom (Berlin, Germany); RNeasy Mini Kit and Quantifast SYBR Green PCR Kit were from Qiagen (Hilden, Germany); iScript cDNA Synthesis Kit was from Bio-Rad (Munich, Germany); ProteoExtract Native Membrane Extraction Kit from VWR International (Bruchsal, Germany); Western Lightning® Plus-ECL from PerkinElmer (Rodgau, Germany). Antibodies: anti-ABCC1 mAb (MRPr1), anti-ABCC2 mAb (M2III-6), anti-ABCC3 mAb (M3II-9), anti-ABCC4 mAb (M4I-80), anti-ABCB1 mAb (C219), anti-ABCG2 mAb (BXP-53) and anti-β-Actin mAb (B11V08) were obtained from Enzo Life Sciences (Lörrach, Germany). Secondary antibodies: horseradish peroxidase-labeled anti-mouse and horseradish peroxidase-labeled anti-rat were purchased from KPL (Wedel, Germany). Calcein AM, CellTracker™ Green CMFDA (5-Chloromethylfluorescein Diacetate) and BODIPY® FL prazosin were from Life Technologies (Darmstadt, Germany); 8-[Fluo]-cAMP (8- (2- [Fluoresceinyl]aminoethylthio)adenosine- 3′, 5′- cyclic monophosphate) (fluo-cAMP) was from BioLog (Bremen, Germany); PSC 833 was a kind gift from Novartis Pharma (Basel, Switzerland); Ko134 was purchased from tebu-bio (Offenbach, Germany); insulin, MK 571, Texas Red® (sulforhodamine 101), rhodamine 123 and fluorescein isothiocyanate-dextran (average MW 3000–5000) (FITC-Dextran 4 kDa) were from Sigma-Aldrich (Taufkirchen, Germany).

Cell culture

HIBCPP cells have previously been derived from a surgically removed human CP papilloma by Ishiwata *et al.* (8). In brief, the cells were taken into culture following enzymatical digestion of papilloma material with subsequent centrifugation of the cells. They grow continuously in culture, display an epithelial arrangement and express keratin and Leu-7 (8). For all experiments HIBCPP cells between passage 34 and 37 were used. They were cultured in DMEM/F-12 supplemented with 5 µg/ml insulin, 4 mM L-glutamine, 100 U/ml penicillin, 100 µg/ml streptomycin and 10% (v/v) FBS. After reaching confluence, cells were incubated with serum-free medium for 24 h.

RNA isolation and quantitative real-time PCR (qPCR)

RNA was extracted from cells from 25 cm^2 flasks according to the protocol of the RNeasy Mini Kit for animal cells using spin technology. RNA concentration was measured with a NanoDrop spectrophotometer (PEQLAB, Erlangen, Germany), 1 µg of RNA was converted into cDNA and 50 ng cDNA were used for real-time PCR. All primers (Table I) were purchased from Invitrogen and were generated with the help of PrimerBank (28–30). Real-time PCR was performed with the Quantifast SYBR Green PCR Kit with the following program: 5 min at 95°C as initial activation step, 40 cycles of 10 s at 95°C and 30 s at 60°C. Amplification was followed by melting curve analysis and the final cooling to 40°C. Cycle threshold (Ct) values of each gene of interest (GOI) were normalized to the reference genes (RG) beta-2-microglobulin

Table I Primers Used for qPCR

Target gene	Forward primer, reverse primer
ABCC1 (MRP1)	CGACATGACCGAGGCTACATT, AGCAGACGATCCACAGCAAAA
ABCC2 (MRP2)	CCCTGCTGTTCGATATACCAATC, TCGAGAGAATCCAGAATAGGGAC
ABCC3 (MRP3)	GATCAGGTTTATCTCCAACCCCA, GATCCCAGTACGAAACTTCACC
ABCC4 (MRP4)	TGTGGCTTTGAACACAGCGTA, CCAGCACACTGAACGTGATAA
ABCC5 (MRP5)	GAACTCGACCGTTGGAATGC, TCATCCAGGATTCTGAGCTGAG
ABCC6 (MRP6)	AGATGGTGCTTGGATTCGCC, GCCACACAGTAGGATGAATGAG
ABCC10 (MRP7)	GTCCAGATTACATCCTACCCTGC, GCCAACACCTCTAGCCCTATG
ABCC11 (MRP8)	GTGAATCGTGGCATCGACATA, GCTTGGGACGGAAGGGAATC
ABCC12 (MRP9)	ATGATGCCGGGCTACTCTC, CAGGGTGTCTACGGTCAGC
ABCB1 (P-GP)	TTGCTGCTTACATTCAGGTTTCA, AGCCTATCTCCTGTCGCATTA
ABCG2 (BCRP)	ACGAACGGATTAACAGGGTCA, CTCCAGACACACCACGGAT
b2M	GAGGCTATCCAGCGTACTCCA, CGGCAGGCATACTCATCTTTT
GAPDH	ATGGGGAAGGTGAAGGTCG, GGGGTCATTGATGGCAACAATA
PBGD	TGCTCGCATACAGACGGAC, GGTAAACAGGCTTTTCTCTCCAA
HPRT	CCTGGCGTCGTGATTAGTGAT, AGACGTTCAGTCCTGTCCATAA

(b2M), glyceraldehyde-3-phosphate dehydrogenase (GAPDH), porphobilinogen deaminase (PBGD) and hypoxanthine phosphoribosyltransferase (HPRT) ($2^{Ct}{}_{RG}{}^{-Ct}{}_{GOI}$).

Protein isolation and Western blot

Membrane proteins were extracted according to the protocol of the ProteoExtract Native Membrane Extraction Kit (Calbiochem®, EMD Millipore / Merck KGaA, Darmstadt, Germany), then they were diluted in 5x sample buffer (37.5% glycerol, 5% sodium dodecyl sulfate (SDS), 0.05% bromphenol blue, 0.225 M TRIS, freshly added: 0.25 M dithiothreitol (DTT)) and denatured. Samples were subjected to electrophoresis (20 min at 80 V and 60 min at 150 V) on 10% SDS polyacrylamide gels and transferred to polyvinylidene difluoride membranes *via* immunoblotting for 1.5 h at 300 mA. Then blots were blocked for 1 h at room temperature (RT) with PBS containing 1% non-fat dry milk powder, 1% bovine serum albumin and 0.05% Tween® 20. Afterwards, incubation with primary antibodies was done overnight at 4°C. Next, blots were incubated with secondary antibodies for 1 h at RT and subsequently protein bands were visualized with Western Lightning® Plus-ECL and detected by Quantity One® software with ChemiDoc™ XRS.

Immunohistochemistry

Immunohistochemistry was basically performed as described (9). HIBCPP cells grown on cell culture filter inserts were washed two times with PBS and subsequently fixed with 4% formaldehyde (w/v in PBS) at room temperature for 10 min, followed by permeabilization with 0.5% Triton X-100 / 1% BSA (v/v in PBS). Immunofluorescence staining was performed using the following primary antibodies: polyclonal rabbit anti-ZO-1 (dilution 1:250; Zymed, San Francisco, USA), monoclonal rat anti-ABCC1 (1:250), monoclonal rat anti-ABCC4 (1:100) and monoclonal mouse anti-ABCB1 (1:100). As secondary antibodies 1:250 dilutions of a chicken anti-rabbit Alexa Flour 488, a donkey anti-rat Alexa Fluor 594 or a donkey anti-mouse Alexa Fluor 594 were used (all from Molecular Probes, Oregon, USA). For actin staining the cells were incubated with phalloidin Alexa Fluor 660 (dilution 1:250; Molecular Probes, Oregon, USA). Nuclei were stained with 4′-6-diamidino-2-phenylindole dihydrochloride (DAPI) (1:50000). Fluorescence images were acquired with a AxioObserver Z1 equipped with Apotome and Zen acquisition software (Carl Zeiss, Jena, Germany) using a 63×/1.4 objective lens. With this system, an optical slice view can be reconstructed from fluorescent samples. Representative selections of images were chosen from multiple standard microscopic fields for graphical presentation.

Uptake experiments

For uptake assays to determine functionality of ABCC1, ABCC4 and ABCB1 cells were seeded in 96 well microplates with a density of 10^5 cells per cm^2 and cultivated for 9 days. Preparatory, cells were washed with Krebs Ringer Buffer (KRB), followed by preincubation with or without (control) inhibitors for 30 min at 37°C. Afterwards, cells were incubated with substrates and inhibitors for 90 min at 37°C. All substances were dissolved in DMSO whereat final DMSO concentration did not exceed 1.25%. In order to terminate substrate transport, cells were washed with ice-cold KRB and then lysed with 1% Triton X-100 in KRB for 30 min at 37°C. Finally, fluorescence was measured by Fluoroskan Ascent™ Microplate Fluorometer (485/520 nm).

To perform the ABCG2 uptake assay, cells were seeded in 25 cm^2 flasks and after washing steps they were preincubated for 15 min at 37°C with or without inhibitor. Then BODIPY® FL prazosin was added, and cells were incubated for another 60 min. Cells only incubated with KRB served as a negative control. Afterwards, cells were washed with ice-cold KRB for termination of substrate transport. Next, cells were trypsinized for detachment and transferred to a tube. Subsequently cells were washed again and resuspended in ice-cold KRB. Finally, fluorescent cells were detected with FACS Calibur™ (488/530 nm).

Permeation studies

HIBCPP cells were grown on Polyester Membrane Transwell® Permeable Supports (Corning, New York, USA) at a seeding density of $3*10^5$ cells per cm^2 and before starting the experiment TEER measurement was performed with cellZscope®. Only filter cultures with a TEER ≥150 Ωcm^2 were used for experiments. TEER measurement as well as transport experiments were carried out in KRB. After regeneration cells were preincubated with or without (control) inhibitor for 30 min at 37°C; inhibitor was added to both apical and basolateral compartment. Next, substrate was added either apical or basolateral, samples were drawn after 30, 60, 90 and 120 min and taken volumes were substituted with KRB. To determine paracellular permeability, FITC-Dextran 4 kDa was added instead of substrates.

Samples were collected in black 96 well microplates, and fluorescence measurement was done with the Infinite® F200 PRO microplate reader (fluo-cAMP, rhodamine 123, BODIPY® FL prazosin and FITC-Dextran 4 kDa: 485/535 nm; Texas Red®: 540/590 nm).

Statistical analysis

Data are presented as mean ± SEM. For statistical analysis one-way ANOVA followed by Dunnett's Multiple Comparison Test or Bonferroni's Multiple Comparison Test, respectively, or student's *t*-test were done. (*P* values < 0.05 *, 0.01 **, 0.001 ***).

RESULTS

TEER measurement and transepithelial permeability marker studies

A crucial attribute to exhibit the physiological function of active transport is a low paracellular permeability for hydrophilic molecules that relates to high TEER values (31). Therefore, TEER values of all filter systems were detected and only those with values ≥150 Ωcm^2 were used for functional assays. Additionally, the apparent permeability coefficient (P_{app}) of FITC-Dextran 4 kDa, a hydrophilic compound, was determined. FITC-Dextran 4 kDa was added from either the apical or basolateral compartment and accumulation was measured at the opposite side. For transport from apical to basolateral chamber (a→b) a P_{app} of $2.24 \pm 0.54 \times 10^{-7}$ was calculated and from basolateral to apical chamber (b→a) $2.10 \pm 0.68 \times 10^{-7}$ indicating very low paracellular flux and a relatively high tightness of the cell monolayers.

RNA expression of ABC transporter quantified by real-time PCR

The expression profile of transport proteins of cells is important to know, if cells are supposed to be used as *in vitro* model to study drug transport, disease states or influence of pollutants. As ABC transporters play a pivotal role for xenobiotic transport at the BCSFB, expression level of ABCC1-6, ABCC10-12 (MRP7-9), ABCB1 and ABCG2 was determined. Therefore, RNA was isolated from HIBCPP cells passage 34, 35, 36 and 37, whereat three samples of each passage were collected.

Highest RNA expression was found for ABCC3 and ABCC2, moderate expression for ABCC6, ABCC1, ABCC10, ABCC12, ABCG2, ABCC5 and ABCC4 and very low expression for ABCB1 and ABCC11. Figure 1 shows the expression level of genes as values according to $2^{\Delta Cp}$.

Protein expression and cellular localization of selected ABC transporters

The expression of ABCC1-4, ABCB1 and ABCG2 was investigated on protein level. Notably, ABCC1 and ABCC4 are transport proteins typically expressed at the basolateral membrane of CP in different species (17–21). Expression level of ABCC2 and ABCC3 was examined since RNA expression was quite high. ABCB1 and ABCG2 are both important in

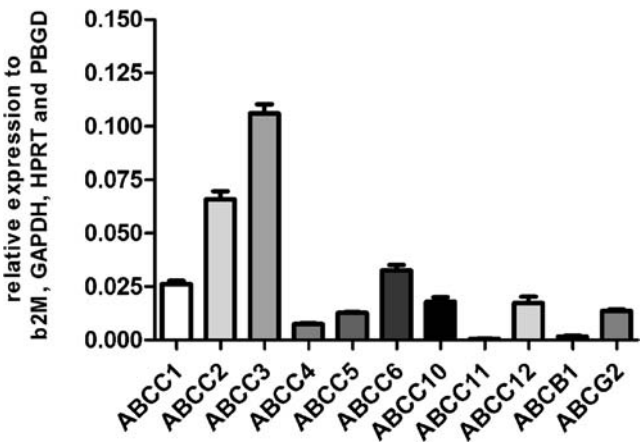

Fig. 1 Relative expression level of ABC transporters. Ct values of each gene were normalized to the geometric mean of Ct values of the reference genes (b2M, GAPDH, HPRT, PBGD) (mean ± SEM).

the formation of multidrug resistance (17), therefore their expression was investigated, too.

Protein bands for all named transporters were detected by Western blotting (Fig. 2). There appeared to be no difference in expression levels between the various passages (Fig. 3). ABCG2 and ABCB1 were detected at ~75 kDa and 150 kDa, respectively. ABCC1, ABCC2, ABCC3 and ABCC4 were detected at ~150 kDa. Figure 2 shows visualized protein bands for all the cell passages and one representative example for β-actin as loading control.

In human CP, ABCC1 and ABCC4 have been detected at the basolateral membrane (18, 21). Expression at the correct membrane side plays a crucial role for maintaining the barrier function. Therefore, localization of these transporters in HIBCPP cells was investigated in this study (Fig. 4). Whereas ABCC1 staining is absent from the apical membrane of the HIBCPP cells (Fig. 4b), ABCC4 displays a rather diffuse staining observed both basolaterally and apically (Fig. 4d). Analysis of ABCB1 suggested that this transporter is diffusely distributed in the cells with some possible subapical location (data not shown).

Functional analysis of cells grown in 96 well microplates

In order to determine whether HIBCPP cells can be used to investigate transport characteristics, uptake assays were carried out with calcein AM, CellTracker™ Green CMFDA, fluo-cAMP and BODIPY® FL prazosin.

Calcein AM permeates cell membranes and inside the cell it is hydrolysed by nonspecific esterases resulting in fluorescent calcein. As calcein is hydrophilic, it is retained in the cell. During membrane passage calcein AM is effluxed by ABCB1 or ABCC1 so that it cannot be cleaved by esterases, and intracellular fluorescence is kept low. Hence, functional activity can be ascertained by using inhibitors of those membrane proteins. Here, PSC 833 was used as P-GP specific inhibitor

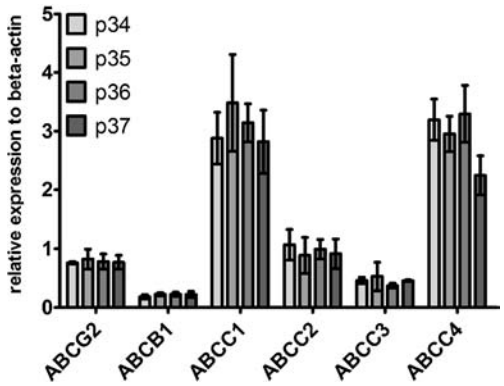

Fig. 3 Expression of ABC transporters relative to β-actin. Expression pattern indicates no difference in between the different passages (mean ± SEM).

and MK 571 as MRP specific inhibitor (Fig. 5a). CellTracker™ Green CMFDA was used to get additional confirmation of ABCC1 activity. This substrate diffuses inside the cell where it is transformed and thus accumulates intracellularly. Accumulation could strongly be increased by addition of MK 571, but also to some extent in presence of PSC 833 (Fig. 5b). Contrary to that, the effect of PSC 833 on transport of calcein AM was significantly higher. For CellTracker™ Green CMFDA, a cumulative effect of PSC 833 and MK 571 was shown, but not for calcein AM.

Fluo-cAMP was used to study ABCC4 functionality as this substance was shown to be a substrate for human ABCC4 (24). Again, PSC 833 and MK 571 were used as inhibitors in the experiment. Both inhibitors had an effect on fluo-cAMP efflux in which MK 571 showed concentration dependency (Fig. 5c). Here, too, a cumulative effect of PSC 833 and MK 571 could be seen.

In order to investigate functionality of ABCG2, an uptake assay with BODIPY® FL prazosin as substrate and Ko134 as BCRP specific inhibitor was carried out (Fig. 5d). A clear difference of uptake in presence and absence of the inhibitor could be seen being indicative for functionality of ABCG2.

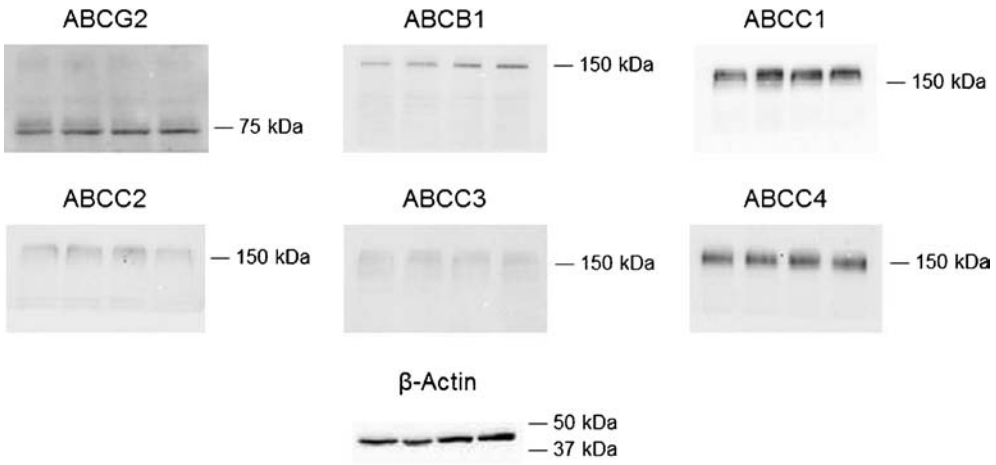

Fig. 2 Protein bands of ABC transporters. Western blot analysis indicate equal protein expression for investigated passages (passage 34–37 from left to right for each protein) Transporters were detected with following antibodies: ABCG2 with BXP-53 (1:75), ABCB1 with C219 (1:100), ABCC1 with MRPr1 (1:100), ABCC2 with M2III-6 (1:50), ABCC3 with M3II-9 (1:50), ABCC4 with M4I 80 (1:100) and β-Actin with B1V08 (1:400). β-Actin served as loading control.

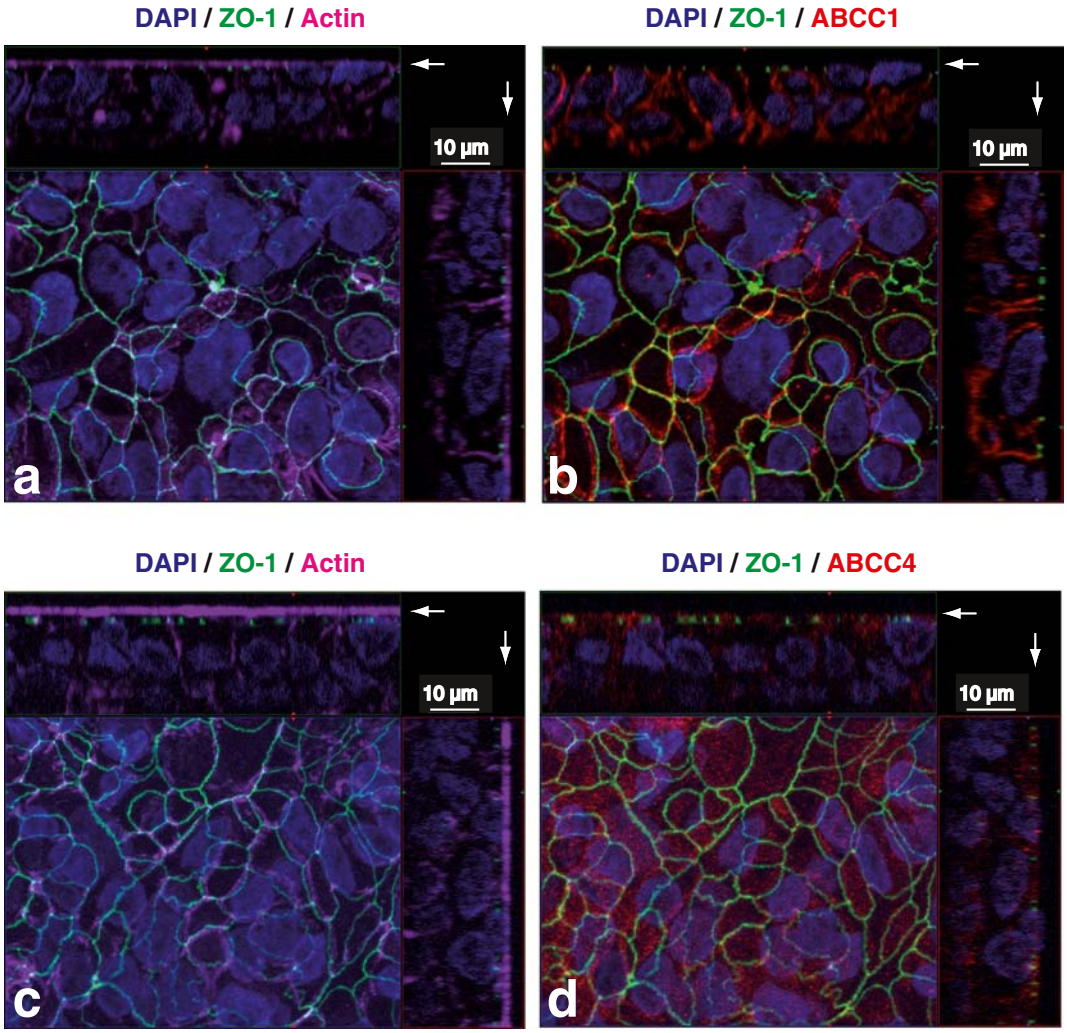

Fig. 4 Localization of ABCC1 and ABCC4 in HIBCPP cells. Expression of ABCC1 (**a**, **b**) and ABCC4 (**c**, **d**) in HIBCPP cells grown in permeable filters is analyzed by immunofluorescence microscopy. Staining of ABCC1 (**b**) and ABCC4 (**d**) are shown in red, the actin cytoskeleton (**a**, **c**) was visualized with phalloidin and is shown in magenta. Detection of tight junctions was performed with an antibody against ZO1 (*green*), staining of cell nuclei was obtained with 4,6-diamidino-2-phenylindole (*blue*). Panels A-D represent Apotome images. The center part of each panel shows an xy en face view of HIBCPP cells grown on cell culture filter inserts. Presented is a maximum-intensity projection through the z-axis of selected slices. The top and right side part of each panel are cross-sections through the z-plane of multiple optical slices. The apical side of HIBCPP cells (indicated by *arrows*) is oriented towards the top of the top part and towards the right of the right side, respectively, of each panel.

Functional analysis of cells grown in 12 well Transwell systems

Another important feature of CP epithelial cells used as *in vitro* model is functional polarity and thus transport of substances in a particular direction across the monolayer. In order to determine the characteristics of the membrane proteins already studied in uptake experiments to this respect, permeation experiments were carried out with cells grown on permeable filter supports with the upper chamber as apical and the lower chamber as basolateral compartment. ABCC1 transport was investigated with Texas Red® as substrate and MK 571 as inhibitor (Fig. 6a). Here, transport of Texas Red® from basolateral to apical compartment was significantly increased in presence of MK 571. Transport from apical to basolateral compartment was slightly decreased, although the difference was not statistically significant. To study ABCC4 transport, MK 571 was used as an inhibitor again, and fluo-cAMP was applied as substrate (Fig. 6b). These experiments showed no statistically significant difference in either direction, but transport of fluo-cAMP from apical to basolateral compartment seemed to be decreased in presence of MK 571. The expression of ABCB1 at CP is still not settled; it appears primarily to be localised subapical (18, 20). For investigation of ABCB1 transport characteristics in HIBCPP cells, the substrate rhodamine 123 and the inhibitor PSC 833 were applied. In these experiments, transport of rhodamine 123 from apical to basolateral compartment showed a significant difference in presence and absence of ABCB1 inhibitor (Fig. 6c). For ABCG2, an apical localization was determined in mouse CP (15) and a subapical localization in rat CP (32). To study ABCG2 transport BODIPY® FL prazosin was added as

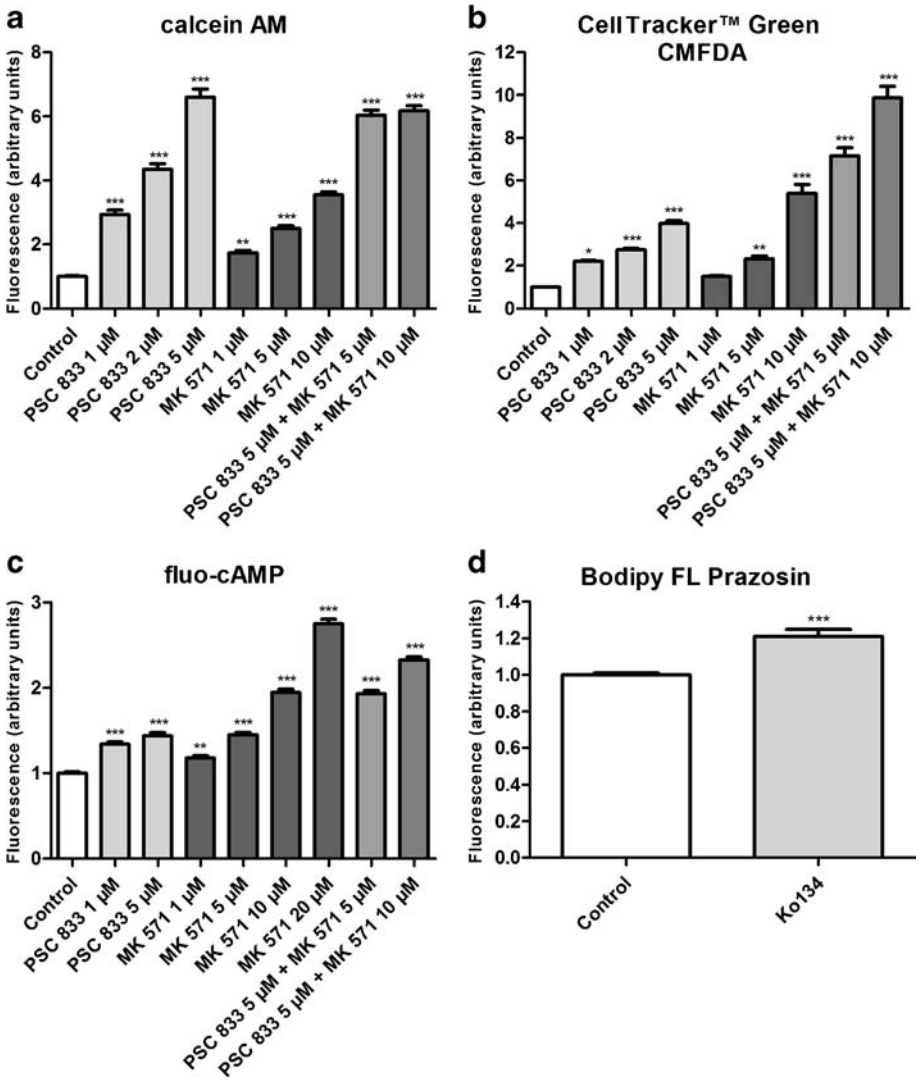

Fig. 5 Uptake experiments for ABCB1, ABCC1, ABCC4 and ABCG2. Control was set to 1 and data are shown as mean ± SEM (*$p < 0.05$, ** $p < 0.01$, *** $p < 0.001$, significantly different from control) ($n = 3$).

substrate and Ko134 as inhibitor. No difference of BODIPY® FL prazosin transport could be detected by incubating HIBCPP cells with or without (control) inhibitor (Fig. 6d).

DISCUSSION

In this study we characterized the HIBCPP cell line for expression and functionality of efflux transport proteins. For this purpose we first confirmed barrier properties of the HIBCPP cells. Schwerk *et al.* have previously detected TEER values around 500 Ωcm^2 for HIBCPP cells grown in permeable filter systems (9). In the present study TEER values detected before starting the experiments were lower, presumably because TEER measurement was done after changing serum-free medium to KRB. Therefore, paracellular transport was investigated with FITC-Dextran 4 kDa. Calculated P_{app} values suggest that HIBCPP cells represent a barrier for this kind of transport. For primary porcine CP epithelial cells, values between $4.56 \pm 0.26 * 10^{-5}$ cm/s and $1.42 \pm 0.13 * 10^{-5}$ cm/s were detected for paracellular marker compounds with a molecular size between 0.4 and 500 kDa (20). The cell line Z310 shows a P_{app} value of $1.28 \pm 0.02 * 10^{-4}$ cm/min ($\approx 2.13 * 10^{-6}$ cm/s) for [^{14}C]inulin (33). Consequently, HIBCPP cells are probably significantly tighter than Z 310 cells and primary porcine CP cells.

Expression of mRNA of ABC transporters known to be expressed in the CP was investigated in the HIBCPP cell line. Interestingly, similarity but also differences to other CP cell lines could be seen: Expression of ABCC1, ABCC2, ABCC3, ABCC4, ABCB1 and ABCG2 could be affirmed. Remarkably, expression of ABCC3 on RNA level is four and 14 times higher than ABCC1 and ABCC4 expression, respectively. Also ABCC2 expression is 2.5 and nine times higher than ABCC1 and ABCC4 expression. Kläs *et al.* found mRNA expression for Abcc1, Abcc4 and Abcb1 in Z310 and TR-CSFB cell lines as well as in primary rat CP cells and in freshly isolated tissue. In TR-CSFB cells Abcc2 mRNA was found,

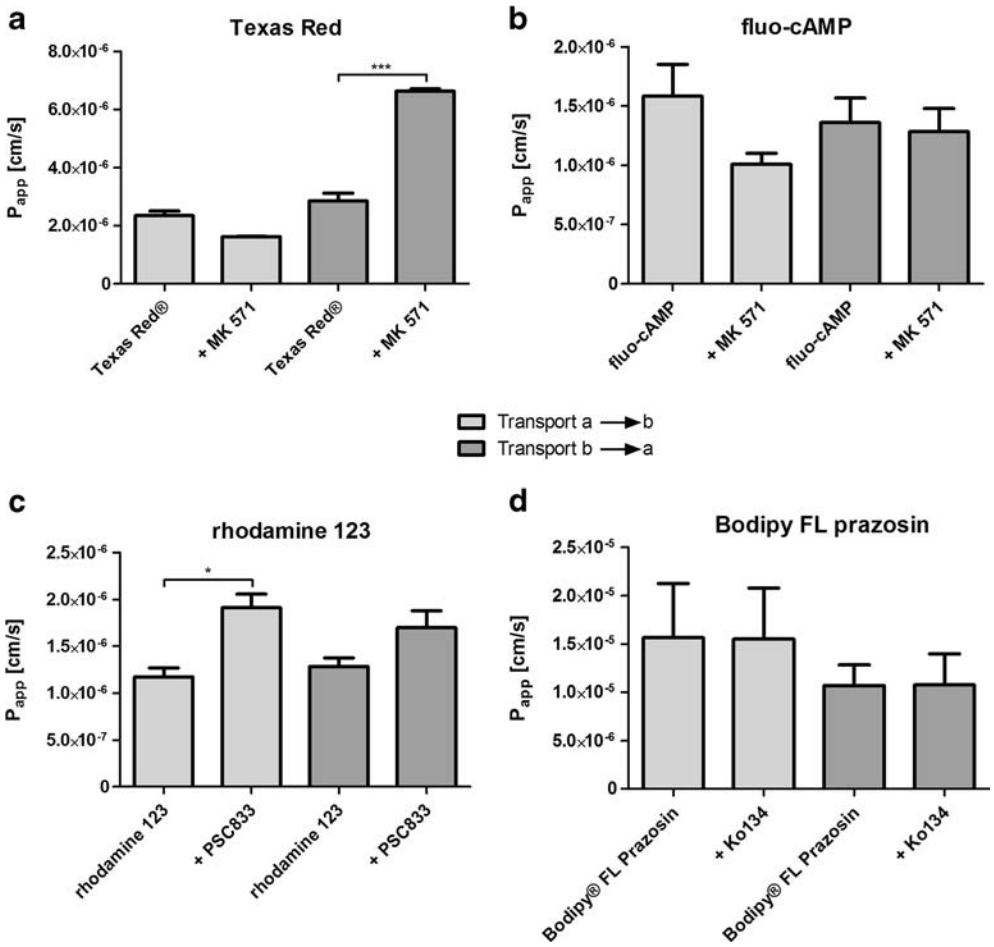

Fig. 6 Permeation experiments with HIBCPP cells grown in permeable filter systems. (**a**) transport of Texas Red as ABCC1 substrate (**b**): transport of the ABCC4 substrate fluo-cAMP (**c**, **d**): transport of ABCB1 substrate (rhodamine123) and ABCG2 substrate (BODIPY® FL prazosin). All experiments were carried out with or without inhibitor and appropriate substrate ($n = 3$). (a⟶b = transport from apical to basolateral compartment, b⟶a = transport from basolateral to apical compartment).

but mRNA of Abcc3 and Abcg2 were hardly detectable (7). Baehr *et al.* (20) investigated mRNA expression of only two ABC transporters, Abcc1 and Abcb1. They found mRNA for both transporters in fresh porcine CP tissue as well as in primary porcine CP cells, whereas mRNA expression level of Abcb1 was low (20). In human CP tissue ABCB1, ABCC1, ABCC2, ABCC3 and ABCC4 expression could be detected (34).

Expression of ABCC1, ABCC2, ABCC3, ABCC4, ABCB1 and ABCG2 could be shown on protein level by means of Western Blot. ABCG2 was detected corresponding to its size at 72 kDa. Protein bands for ABCC1, ABCC2, ABCC3, ABCC4 and ABCB1 were found nearby the 150 kDa band of the marker. As ABCB1 and ABCC4 are detected at ~170 kDa, in general, and ABCC1, ABCC2 and ABCC3 at ~190 kDa, all membrane proteins were detected appropriate to their sizes. Furthermore the proportion of ABCB1 to ABCC1 was correct; the band of ABCC1 was found above that of ABCB1. Additionally, ABCC4 was detected in between these two bands.

The uptake experiments showed functionality of ABCB1, ABCC1, ABCC4 and ABCG2 in HIBCPP cells. Moreover, transport characteristics of HIBCPP cells grown on permeable filter inserts were investigated. Employing this setup, we could show that ABCC1 prevents transport of xenobiotics into the CSF: inhibition of ABCC1 with MK 571 led to a significant increased transport of Texas Red® into the apical compartment. In addition, we could show basolateral localization of ABCC1 by means of immunohistochemistry. This fact supports polarity of HIBCPP cells grown in permeable filter inserts, which had been demonstrated before by polarized localization of E-cadherin and the receptor Met (11).

A special feature of ABCC4 is its expression both at the apical and at the basolateral membrane, depending on the tissue. In CP epithelium of different species it was found to be localised at the basolateral membrane (18, 19, 21). The latter could not be confirmed in this study, immunohistological staining rather showed a diffuse distribution of ABCC4 in HIBCPP cells. Moreover, different to ABCC1 transport properties, the results of these experiments gave no indication for a preferred transport by ABCC4 in either direction. Presumably, this transport protein is not expressed only basolaterally as usually in human CP epithelial cells. Regarding ABCB1 transport properties, a significant difference by inhibition of this membrane protein compared to control was detected for transport from apical to basolateral

compartment, even though it was not as pronounced as for ABCC1. Concerning ABCB1 functionality in CP, there are conflicting results: Baehr *et al.* could detect Abcb1 activity neither in uptake nor in permeation experiments with primary CP epithelial cells from porcine brain (20). Contrary, Kläs *et al.* have shown Abcb1 activity in uptake assays with both cell lines TR-CSFB and Z310 (7). Furthermore, Rao and his group could also show that Abcb1 forms a transport barrier at the apical membrane side in cells of the BCSFB (18). Investigation of ABCG2 functionality gave no indication that this membrane protein is active. Despite this latter observation, the high TEER values, the calculated P_{app} values and the measured transport properties support the applicability of HIBCPP cells as *in vitro* model of the BCSFB.

CONCLUSION

The human CP cell line HIBCPP appears to be an appropriate *in vitro* model for transport studies at the BCSFB. Typical transport proteins of CP are expressed on RNA and protein level. Moreover, transport experiments performed during this study proved functionality for ABCC1, ABCC4, ABCB1 and ABCG2. Consequently, HIBCPP cells promise to be helpful for investigation of carrier-mediated transport processes at the BCSFB.

ACKNOWLEDGMENTS AND DISCLOSURES

The authors thank Carolin Stump-Guthier and Dr. Julia Borkowski for excellent technical assistance.

REFERENCES

1. Spector R, Johanson CE. The mammalian choroid plexus. Sci Am. 1989;261(5):68–74.
2. Gao B, Meier PJ. Organic anion transport across the choroid plexus. Microsc Res Tech. 2001;52(1):60–4.
3. Haselbach M, Wegener J, Decker S, Engelbertz C, Galla HJ. Porcine choroid plexus epithelial cells in culture: regulation of barrier properties and transport processes. Microsc Res Tech. 2001;52(1):137–52.
4. Schroten M, Hanisch F, Quednau N, Stump C, Riebe R, Lenk M, et al. A novel porcine in vitro model of the blood-cerebrospinal fluid barrier with strong barrier function. PLoS One. 2012;7(6):e39835.
5. Kitazawa T, Hosoya K, Watanabe M, Takashima T, Ohtsuki S, Takanaga H, *et al.* Characterization of the amino acid transport of new immortalized choroid plexus epithelial cell lines: a novel in vitro system for investigating transport functions at the blood-cerebrospinal fluid barrier. Pharm Res. 2001;18(1):16–22.
6. Zheng W, Zhao Q. Establishment and characterization of an immortalized Z310 choroidal epithelial cell line from murine choroid plexus. Brain Res. 2002;958(2):371–80.
7. Kläs J, Wolburg H, Terasaki T, Fricker G, Reichel V. Characterization of immortalized choroid plexus epithelial cell lines for studies of transport processes across the blood-cerebrospinal fluid barrier. Cerebrospinal Fluid Res. 2010;7:11.
8. Ishiwata I, Ishiwata C, Ishiwata E, Sato Y, Kiguchi K, Tachibana T, et al. Establishment and characterization of a human malignant choroids plexus papilloma cell line (HIBCPP). Hum Cell. 2005;18(1):67–72.
9. Schwerk C, Papandreou T, Schuhmann D, Nickol L, Borkowski J, Steinmann U, et al. Polar invasion and translocation of Neisseria meningitidis and Streptococcus suis in a novel human model of the blood-cerebrospinal fluid barrier. PLoS One. 2012;7(1):e30069.
10. Schneider H, Weber CE, Schoeller J, Steinmann U, Borkowski J, Ishikawa H, et al. Chemotaxis of T-cells after infection of human choroid plexus papilloma cells with Echovirus 30 in an in vitro model of the blood-cerebrospinal fluid barrier. Virus Res. 2012;170(1–2):66–74.
11. Gründler T, Quednau N, Stump C, Orian-Rousseau V, Ishikawa H, Wolburg H, *et al.* The surface proteins InlA and InlB are interdependently required for polar basolateral invasion by Listeria monocytogenes in a human model of the blood-cerebrospinal fluid barrier. Microbes Infect. 2013;15(4):291–301.
12. Steinmann U, Borkowski J, Wolburg H, Schröppel B, Findeisen P, Weiss C, *et al.* Transmigration of polymorphnuclear neutrophils and monocytes through the human blood-cerebrospinal fluid barrier after bacterial infection in vitro. J Neuroinflammation. 2013;10:31.
13. Borkowski J, Li L, Steinmann U, Quednau N, Stump-Guthier C, Weiss C, et al. Neisseria meningitidis elicits a pro-inflammatory response involving IκBζ in a human blood-cerebrospinal fluid barrier model. J Neuroinflammation. 2014;11(1):B71.
14. Choudhuri S, Cherrington NJ, Li N, Klaassen CD. Constitutive expression of various xenobiotic and endobiotic transporter mRNAs in the choroid plexus of rats. Drug Metab Dispos. 2003;31(11):1337–45.
15. Tachikawa M, Watanabe M, Hori S, Fukaya M, Ohtsuki S, Asashima T, et al. Distinct spatio-temporal expression of ABCA and ABCG transporters in the developing and adult mouse brain. J Neurochem. 2005;95(1):294–304.
16. Urquhart BL, Kim RB. Blood–brain barrier transporters and response to CNS-active drugs. Eur J Clin Pharmacol. 2009;65(11):1063–70.
17. de Lange ECM. Potential role of ABC transporters as a detoxification system at the blood-CSF barrier. Adv Drug Deliv Rev. 2004;56(12):1793–809.
18. Rao VV, Dahlheimer JL, Bardgett ME, Snyder AZ, Finch RA, Sartorelli AC, et al Choroid plexus epithelial expression of MDR1 P glycoprotein and multidrug resistance-associated protein contribute to the blood-cerebrospinal-fluid drug-permeability barrier. Proc Natl Acad Sci U S A. 1999;96(7):3900–5.
19. Frans GMR, Koenderink JB, Masereeuw R. Multidrug resistance protein 4 (MRP4/ABCC4): a versatile efflux transporter for drugs and signalling molecules. Trends Pharmacol Sci. 2008;29(4):200–7.
20. Baehr C, Reichel V, Fricker G. Choroid plexus epithelial monolayers–a cell culture model from porcine brain. Cerebrospinal Fluid Res. 2006;3:13.
21. Leggas M, Adachi M, Scheffer GL, Sun D, Wielinga P, Du G, et al. Mrp4 confers resistance to topotecan and protects the brain from chemotherapy. Mol Cell Biol. 2004;24(17):7612–21.
22. Breen CM, Sykes DB, Baehr C, Fricker G, Miller DS. Fluorescein-methotrexate transport in rat choroid plexus analyzed using confocal microscopy. Am J Physiol Renal Physiol. 2004;287(3):F562–569.
23. Gong Y, Duvvuri M, Krise JP. Separate roles for the Golgi apparatus and lysosomes in the sequestration of drugs in the multidrug-resistant human leukemic cell line HL-60. J Biol Chem. 2003;278(50):50234–9.

24. Reichel V, Masereeuw R, van den Heuvel JJMW, Miller DS, Fricker G. Transport of a fluorescent cAMP analog in teleost proximal tubules. Am J Physiol Regul Integr Comp Physiol. 2007;293(6):R2382–2389.
25. Fardel O, Lecureur V, Daval S, Corlu A, Guillouzo A. Up-regulation of P-glycoprotein expression in rat liver cells by acute doxorubicin treatment. Eur J Biochem. 1997;246(1):186–92.
26. Robey RW, Honjo Y, van de Laar A, Miyake K, Regis JT, Litman T, et al. A functional assay for detection of the mitoxantrone resistance protein, MXR (ABCG2). Biochim Biophys Acta Biomembr. 2001;1512(2):171–82.
27. Allen JD, van Loevezijn A, Lakhai JM, van der Valk M, van Tellingen O, Reid G, et al. Potent and specific inhibition of the breast cancer resistance protein multidrug transporter in vitro and in mouse intestine by a novel analogue of fumitremorgin C. Mol Cancer Ther. 2002;1(6):417–25.
28. Spandidos A, Wang X, Wang H, Seed B. PrimerBank: a resource of human and mouse PCR primer pairs for gene expression detection and quantification. Nucleic Acids Res. 2010;38(Database issue):D792–799.
29. Wang X, Seed B. A PCR primer bank for quantitative gene expression analysis. Nucleic Acids Res. 2003;31(24):e154.
30. Wang X, Spandidos A, Wang H, Seed B. PrimerBank: a PCR primer database for quantitative gene expression analysis, 2012 update. Nucleic Acids Res. 2012;40(Database issue):D1144–1149.
31. Gath U, Hakvoort A, Wegener J, Decker S, Galla HJ. Porcine choroid plexus cells in culture: expression of polarized phenotype, maintenance of barrier properties and apical secretion of CSF-components. Eur J Cell Biol. 1997;74(1):68–78.
32. Halwachs S, Lakoma C, Schäfer I, Seibel P, Honscha W. The antiepileptic drugs phenobarbital and carbamazepine reduce transport of methotrexate in rat choroid plexus by down-regulation of the reduced folate carrier. Mol Pharmacol. 2011;80(4):621–9.
33. Shi LZ, Li GJ, Wang S, Zheng W. Use of Z310 cells as an in vitro blood-cerebrospinal fluid barrier model: tight junction proteins and transport properties. Toxicol In Vitro. 2008;22(1):190–9.
34. Niehof M, Borlak J. Expression of HNF4alpha in the human and rat choroid plexus: implications for drug transport across the blood-cerebrospinal-fluid (CSF) barrier. BMC Mol Biol. 2009;10:68.